ARTICLE IN PRESS



Available online at www.sciencedirect.com

ScienceDirect

Geochimica et Cosmochimica Acta xxx (2019) xxx-xxx

Geochimica et Cosmochimica Acta

www.elsevier.com/locate/gca

Refining the planktic foraminiferal I/Ca proxy: Results from the Southeast Atlantic Ocean

Wanyi Lu^a, Alexander J. Dickson^b, Ellen Thomas^{c,d}, Rosalind E.M. Rickaby^e
Piers Chapman^f, Zunli Lu^{a,*}

^a Department of Earth Sciences, Syracuse University, Syracuse, NY, USA
^b Department of Earth Sciences, Royal Holloway University of London, Egham, UK
^c Department of Geology and Geophysics, Yale University, New Haven, CT, USA
^d Department of Earth and Environmental Sciences, Wesleyan University, Middletown, CT, USA
^e Department of Earth Sciences, University of Oxford, Oxford, UK
^f Department of Oceanography, Texas A&M University, College Station, TX, USA

Received 3 June 2019; accepted in revised form 17 October 2019; available online xxxx

Abstract

Profound changes in upper ocean oxygenation have taken place in recent decades and are expected to continue in the future, but the complexity of the processes driving these changes has yet to be fully unraveled. Planktic foraminiferal I/Ca is a promising tool to reconstruct the extent of past upper ocean oxygenation, but a thorough assessment is necessary to evaluate both its potential and its limitations. We used foraminifers from Holocene core-tops (Southeast Atlantic Ocean) to document planktic I/Ca across a range of oceanographic conditions. Subsurface O_2 concentrations may be the dominant control on planktic foraminiferal I/Ca and planktic I/Ca decreases rapidly at low O_2 conditions ($O_2 < \sim 70-100 \,\mu\text{mol/kg}$). We thus document that low planktic I/Ca can be used empirically to indicate hypoxia in the upper water column, but questions remain as to the mechanistic understanding of the relation between seawater iodine speciation change, its O_2 threshold and foraminiferal I/Ca. Planktic I/Ca records from core GeoB1720-2 (Benguela Upwelling System, SE Atlantic) suggest that hypoxic waters were present near the site persistently during the last 240 ka, without clear glacial-interglacial variability.

Keywords: Planktic foraminifera; I/Ca; Upper Ocean; Hypoxia

1. INTRODUCTION

The carbonate I/Ca proxy as used on planktic foraminifera has great potential to reconstruct upper ocean oxygenation changes, for which few proxies are available (Lu et al., 2016, 2018; Hoogakker et al., 2018). Inorganic iodine in the oceans exists as two thermodynamically stable species: iodate (IO₃⁻, oxidized form) and iodide (I⁻, reduced form), and the equilibration between the two species is highly redox-sensitive.

* Corresponding author. *E-mail address:* zunlilu@syr.edu (Z. Lu).

https://doi.org/10.1016/j.gca.2019.10.025 0016-7037/© 2019 Elsevier Ltd. All rights reserved. Iodate is completely reduced to iodide in anoxic waters, and re-oxidized under well-oxygenated conditions (Rue et al., 1997). Only IO_3^- is incorporated into the calcite structure (Lu et al., 2010) by substituting for the CO_3^{2-} ion (Podder et al., 2017; Feng and Redfern, 2018). Higher foraminiferal I/Ca values thus generally record higher IO_3^- concentrations in seawater, and therefore indicate better-oxygenated water conditions. Planktic foraminiferal I/Ca has been shown to primarily record upper ocean oxygenation (Zhou et al., 2014; Lu et al., 2016; Hoogakker et al., 2018). A threshold value (I/Ca < \sim 2.5 μ mol/mol) was proposed to indicate low O_2 upper ocean waters, based on a limited number of globally-distributed core-top foraminiferal samples (Lu et al., 2016).

We collected more core-top data to further elucidate the behavior of I/Ca across different oxygenation windows: anoxic $(O_2 = 0)$, suboxic $(O_2 < 10 \,\mu\text{mol/kg})$, hypoxic $(O_2 < \sim 70-100 \,\mu\text{mol/kg})$, and oxic $(O_2 > 100 \,\mu\text{mol/kg})$.

Planktic I/Ca and bulk sediment nitrogen isotopes $(\delta^{15}N)$ both have been used to indicate low O_2 conditions in the upper water column. One of the motivations of this study is to compare and differentiate the behavior of planktic I/Ca and bulk δ^{15} N across hypoxic and suboxic windows. In suboxic waters (e.g., eastern tropical Pacific and Arabian Sea), water column denitrification preferentially removes ¹⁴N, leaving the residual nitrate enriched in ¹⁵N, thus bulk $\delta^{15}N$ is interpreted to reflect the relative degree of water column denitrification under suboxic conditions (Altabet et al., 1999; Robinson et al., 2009; Galbraith et al., 2013). In areas of incomplete nitrate consumption on surface waters (e.g., high nutrient regions), bulk δ^{15} N signals are generally thought to reflect relative degrees of nitrate utilization by the phytoplankton community (Pichevin et al., 2005b; Galbraith et al., 2008; Galbraith and Jaccard, 2015). Therefore, a study of planktic foraminiferal I/Ca in low oxygen regions of the Atlantic where there is no water column denitrification should provide new insights into these two oxygen proxies targeting a similar part of the water column.

Ocean deoxygenation has been observed in large areas of the Southeast Atlantic Ocean in the past five decades (Schmidtko et al., 2017). Previous studies reconstructed glacial-interglacial histories of sea surface temperature (SST) (e.g., Farmer et al., 2005; Pichevin et al., 2005a; Mollenhauer et al., 2003) and primary productivity (e.g., Mollenhauer et al., 2002; Romero et al., 2015), but few studies focused on reconstructing water column oxygenation (e.g., McKay et al., 2016). Information on glacial-interglacial changes in oceanic oxygenation may help inform us on the extent of and controls on potential future ocean deoxygenation.

We report I/Ca data on eight planktic foraminiferal species (depth habitats from near-surface to the thermocline) in 19 core-tops from the Southeast Atlantic Ocean (Southwest African margin, Fig. 1). We aim to better constrain the signal of planktic foraminifera I/Ca in hypoxic as compared to suboxic hydrographic regimes. In addition, we show a downcore I/Ca record of GeoB1720-2 (28°59′S, 13°50′E, 1997 m) within the Benguela Upwelling System (BUS), and compare it to a bulk sediment $\delta^{15}N$ record from the BUS (Pichevin et al., 2005b) to reconstruct the upper water column conditions over the last two glacial cycles.

2. SAMPLES AND METHODS

2.1. Study site

The Southeast Atlantic Ocean is a region with severe low oxygen conditions linked to upwelling of nutrient rich waters and the resulting high productivity, particularly in the BUS (Chapman and Shannon, 1985; Jarre et al., 2015). The BUS is bounded to the North by the Angola-Benguela frontal zone (between 14 and 17°S), to the South by the Agulhas retroflection (around 37°S) (Shannon and

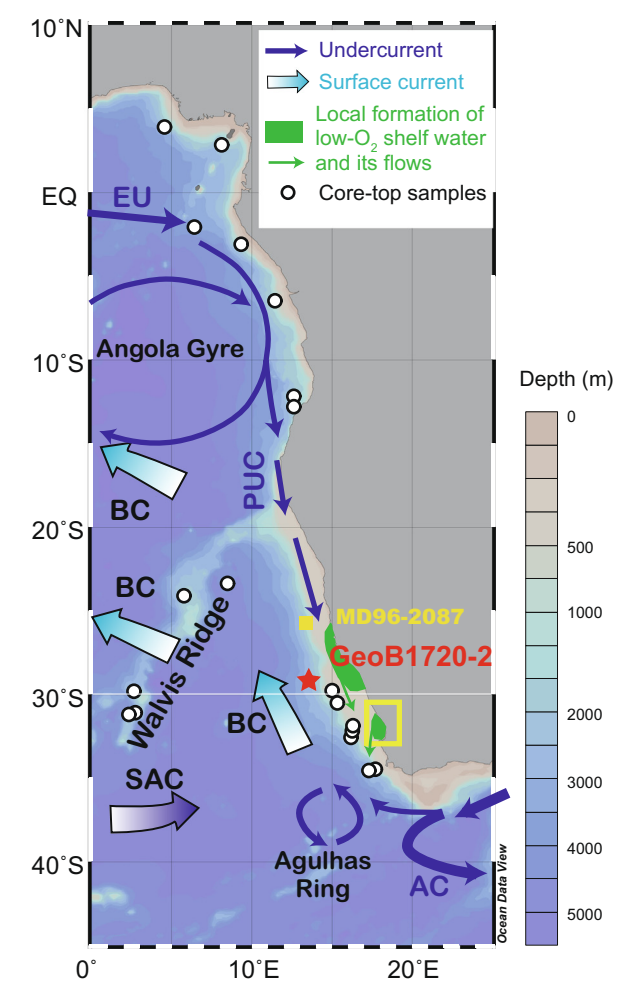


Fig. 1. Locations of core-top samples and site GeoB1720-2. The yellow box marks the sampling area of dissolved iodate and O₂ concentrations in seawater in the Southern BUS region in Fig. 5b (Chapman, 1983). The yellow square marks site MD96-2087 in Fig. 6, for comparison with I/Ca records. The upper ocean circulation in the Southeast Atlantic Ocean is modified after Chapman and Shannon (1985) and Stramma and England (1999). EU: Equatorial Undercurrent; PUC: Poleward Undercurrent; BC: Benguela Current; SAC: South Atlantic Current; AC: Agulhas Current. (For interpretation of the references to colour in this figure legend, the reader is referred to the web version of this article.)

Nelson, 1996), and is one of the most highly productive regions in the world oceans. Wind-driven upwelling of nutrient-rich waters along the west coast of southern Africa is important for marine biodiversity and food production (Chapman and Shannon, 1985; Jarre et al., 2015). Mutually inconsistent observations have been made indicating the occurrence of (Hutchings et al., 2009) or lack of (Pitcher et al., 2014) long-term oxygen decline in the coastal waters in the BUS since the 1960s.

Shelf water along the west coast of southern Africa commonly contains low dissolved O_2 (e.g., <2 ml/l, approximately $<90 \mu mol/kg$), and the O_2 concentrations vary significantly spatially (Figs. 1 and 2). Upper ocean waters

close to the southwest African coast are affected by both the southward Poleward Undercurrent (PUC), down to 200 m depth along the shelf break, and by the northward Benguela Current, further offshore, down to 1200 m depth. The Benguela Current forms the eastern limb of the South Atlantic gyre, and contains water from the South Atlantic Current with additional inputs of warm, salty Indian Ocean water from the Agulhas Current (Stramma and England, 1999). The PUC originates from the Equatorial Undercurrent and the Angola Gyre, and transports low oxygen waters southward along the shelf north of 27°S (Fig. 1). The low O2 conditions of the BUS in the coastal area between 30°S and 34°S are most likely due to local decomposition of organic matter (Chapman and Shannon, 1985) (Figs. 1 and 2).

Site GeoB1720-2 is located on the Southwest African slope within the northward path of the Benguela Current (Figs. 1 and 2). The upper ocean hydrography over this site is affected by the upwelling of South Atlantic Central Water close to the African coast, Agulhas leakage of tropical Indian Ocean waters, and subantarctic waters from large-scale eddy mixing at the subtropical front (~42°S) (Stramma and England, 1999; Dickson et al., 2010).

2.2. Samples materials

A total of 19 core-top samples were obtained from the upper 5 cm of cores from the Lamont-Doherty Core Repository (Table S1). The core-top sediments were wet-sieved to the >63 µm fraction with MilliQ water, then oven-dried at 40 °C. Specimens from eight planktic foraminiferal species (Globigerinoides ruber, Neogloboquadrina incompta, Globigerina bulloides, Globorotalia truncatulinoides (sinistral and dextral), Globigerinoides sacculifer, Globorotalia inflata, Neogloboquadrina dutertrei, and Globorotalia menardii) were picked, and 25–80 individuals from the 150–300 µm size fraction were used for I/Ca analyses. Two species, G. truncatulinoides (sinistral) and N. incompta, were picked from sieved sediments from core GeoB1720-2. Around 25 specimens of G. truncatulinoides (sinistral) and ~80 speci-

mens of N. incompta from 150 to 300 μ m size fraction were used for I/Ca analyses.

2.3. Age model

Radiocarbon dating of the planktic foraminifer G. inflata from selected samples shows a Holocene age (Table S1). Radiocarbon was analyzed at the Keck Carbon Cycle AMS Facility at University of California, Irvine. The age model of core GeoB1720-2 is based on nine AMS ¹⁴C dates between 0 and 200 cm depth for the planktic foraminifer G. inflata (Dickson et al., 2009), and is extended downcore by tying the N. incompta δ^{18} O stratigraphy to the global benthic foraminiferal δ^{18} O stack (Lisiecki and Raymo, 2005) between 200 and 900 cm depth (Fig. S1 and Table S2), assuming the GeoB1720-2 δ^{18} O record can be correlated to the global stack. The N. incompta δ^{18} O data for core GeoB1720-2 are here first reported. They were measured on the 150 - 250 µm size fraction from homogenized sample sizes of ~20 individuals on a Thermo MAT Delta V Advantage mass spectrometer coupled to a Kiel Device at the Department of Earth Sciences, University of Cambridge, and the Department of Physical Sciences, The Open University. Calibration to Vienna Pee Dee Belemnite was via NBS19 standards. Precision is $\pm 0.1\%$ (1 S.D.).

2.4. Foraminiferal I/Ca analyses

The foraminiferal I/Ca analytical methods follow Lu et al. (2016). The samples were gently crushed with cleaned glass slides to open all chambers of the tests. Samples were cleaned by ultrasonication in MilliQ water to remove clays, a 10-minute boiling-water bath in NaOH-buffered $1\%~H_2O_2$ solutions to remove organic matter, and 3 additional rinses with MilliQ water. The cleaned samples were dissolved in $3\%~HNO_3$, and diluted to solutions with $\sim \! 50~ppm$ Ca for analyses. A 0.1%~tertiary amine solution was added to stabilize iodine in solution. The measurements were performed immediately, to minimize potential iodine loss due to iodine

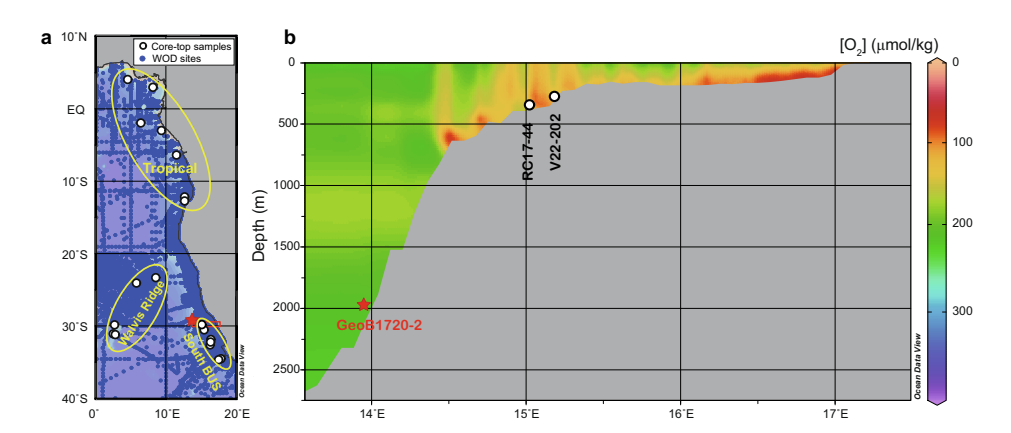


Fig. 2. (a) Seawater CTD [O₂] profile locations in the study area, World Ocean Database (WOD) 2013 (Boyer et al., 2013). We divided our dataset into three regions, as outlined by the yellow ellipses. (b) Cross-section (red box with latitudes between 28°45′ S and 29°15′ S) shows site GeoB1720-2 on the continental slope, and the location of two cores in the coastal area of the BUS, showing significant spatial variation of O₂ concentrations.

speciation change and volatilization. The I/Ca analyses were performed on a quadrupole ICP-MS (Bruker M90) at Syracuse University. The sensitivity of I-127 is tuned to 100-120 kcps for a 1 ppb standard. The reference standard JCp-1 (I/Ca value of 4.27 µmol/mol) was analyzed repeatedly to monitor long-term accuracy (Lu et al., 2010). The detection limit of I/Ca is on the order of 0.1 µmol/mol. Replicates of selected *G. truncatulinoides* (sinistral) from core GeoB1720-2 yielded a reproducibility ranging from $\pm 3\%$ (0.03 µmol/mol; 1σ) to $\pm 10\%$ (0.15 µmol/mol; 1σ) for I/Ca (Table S3).

2.5. Planktic foraminiferal habitat

Calcification depths where the average geochemical signal is locked into the planktic foraminiferal shell are usually estimated from comparison of $\delta^{18}O$ of foraminifera with that of equilibrium calcite, based on historical temperature and salinity data (Anand et al., 2003). Calcification depths for several of the species used in this study have been calibrated to depth habitats of ~ 100 m (summer) and ~ 80 m (winter) for *N. incompta*; and ~ 340 m (summer) and ~ 300 m (winter) for *G. truncatulinoides* (dextral) in multicore GeoB1720-3 (28°59′S, 13°50′E, 2004 m) (Dickson et al., 2010). This core is located within a few meters of GeoB1720-2, thus the data are broadly applicable to our study region.

2.6. Hydrographic data

Oxygen data for core-top sites were obtained from highresolution CTD profiles in the World Ocean Database (WOD) 2013 (https://www.nodc.noaa.gov/OC5/WOD/ pr_wod.html) (Boyer et al., 2013) (Fig. 2a). We divided the studied area into three geographic regions: a tropical region at latitudes between 5°N and 15°S; a Southern BUS region at latitudes between 30°S and 35°S; and a Walvis Ridge region at latitudes between 23°S and 32°S (Fig. 2a). Many of the core-top samples are in areas with great spatial variability in O2 conditions, thus we determined the minimum O2 concentrations in the water column from the nearest location, and within an $0.25^{\circ} \times 0.25^{\circ}$ area of the core-top samples in WOD2013. Minimum O₂ in the water column is used because O2 has to drop below a certain threshold to trigger iodate reduction, recorded as low foraminiferal I/Ca (Lu et al., 2016). Minimum O₂ values generally occur in the bottom waters over the shelf, but are found in mid-water off the shelf. Minimum O₂ maps were produced using Ocean Data View's gridding tool, and the individual minimum O₂ values were calculated using the statistics tool in that program (Schlitzer, 2018).

3. RESULTS

Low core-top I/Ca values ($<\sim$ 2.5 µmol/mol), regardless of species, are observed in the tropical and Southern BUS regions, which generally contain hypoxic waters at middepths or bottom depths ($O_2 < \sim$ 70–100 µmol/kg) (Figs. 3 and 4). High core-top I/Ca values ($>\sim$ 4 µmol/mol), regard-

less of species, are found in the Walvis Ridge region, where waters generally are well oxygenated ($O_2 > \sim 100 \mu mol/kg$).

We do not observe any consistent or systematic differences in I/Ca between symbiont-bearing species (G. ruber and G. sacculifer) and symbiont-barren species (G. menardii, N. dutertrei, N. incompta, G. bulldoides, G. inflata, G. truncatulinoides) within the same core-top sample (Fig. S2). At Southern BUS (low oxygen region), symbiont-barren species record slightly wider ranges of I/Ca and the average I/Ca of symbiont-barren species are lower than the average values of symbiont-bearing species in two out of three core-top samples. In the high oxygen Walvis Ridge region, I/Ca values in three out of four samples show similar ranges and variabilities in symbiotic vs. non-symbiotic species, except for one sample with notably smaller variability in symbiotic species.

Higher core-top I/Ca values are generally associated with higher O_2 conditions in the water column as estimated from the nearest site in the WOD2013 database (Fig. 5), consistent with Lu et al. (2016). At three sites in the Southern BUS region (V19-238, V19-228, and V14-70, see Table S1 for details), however, high modern minimum O_2 concentrations (150–220 µmol/kg) apparently are associated with low I/Ca (\sim 2 µmol/mol), but the O_2 values around these core-top sites are highly variable spatially (Fig. 2).

In the downcore record of GeoB1720-2, almost all G. truncatulinoides (sinistral) and N. incompta I/Ca values are <2.5 µmol/mol during the last two glacial cycles (Fig. 6).

4. DISCUSSION

4.1. Subsurface O₂ conditions

Measurements of the core-top samples in the Southeast Atlantic Ocean confirmed that low planktic I/Ca values can reveal the presence of low- O_2 waters in the upper ocean (Fig. 5c), as previously demonstrated (Lu et al., 2016). However, we also found high O_2 – low I/Ca values in the Southern BUS region (Fig. 5c), which may be explained by different scenarios: (1) O_2 values from the WOD2013 do not represent the actual conditions during foraminiferal growth, due to short-term or spatial variability of O_2 ; (2) the foraminifera calcified in high O_2 – low IO_3 water, due to slow kinetics of I^- oxidation; (3) the planktic foraminifera lived at nearby locations with lower O_2 and were transported to their current sites (Fig. 2); (4) unknown factors are limiting IO_3^- uptake by foraminifera at these sites.

Examining the first of these possibilities, hypoxic waters are common in the shelf areas of the BUS system and their extent and level of oxygen depletion vary spatially and on seasonal, interannual, and decadal timescales (Jarre et al., 2015). Significant vertical and seasonal changes in water column oxygen concentrations are more likely in the near-shore than in the offshore regions (Lamont et al., 2015; Pitcher et al., 2014). However, episodic hypoxic conditions in the water column have been reported offshore of the BUS (Pitcher et al., 2014), and may provide low O₂ water at our

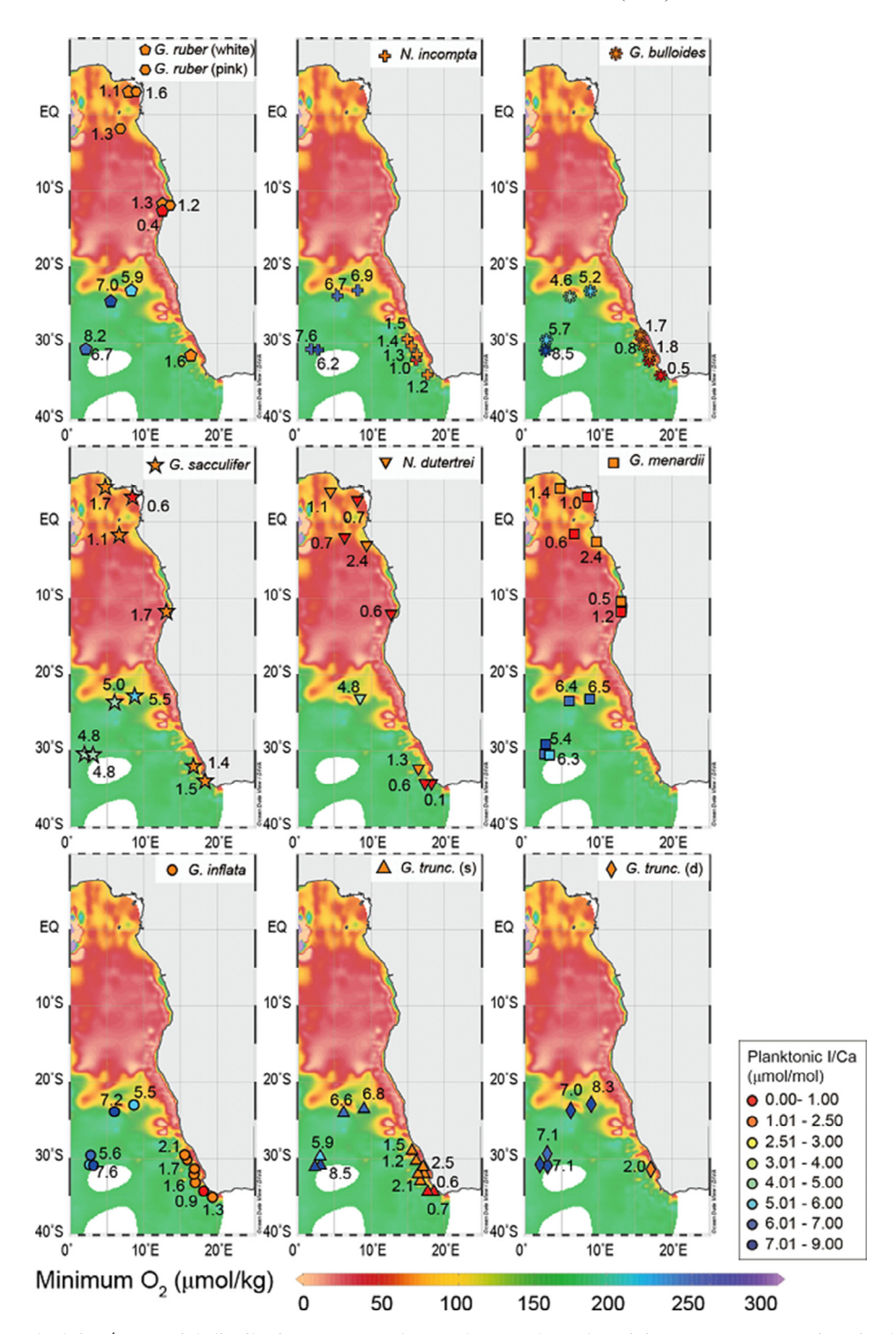


Fig. 3. Core-top planktic I/Ca spatial distribution maps. Background maps show the minimum O_2 concentrations in the water column. Numbers next to the symbols show the planktic I/Ca values.

core-top sites not captured in the WOD2013 dataset, which does not comprise seasonal or annual $\rm O_2$ measurements in the Southern BUS region. The $\rm O_2$ data in WOD2013 also span a considerable time period, representing an additional source of uncertainty. Thus the uncertainty arising from modern measurements of $\rm O_2$ and its short-term variability may at least partially explain the high $\rm O_2$ – low I/Ca cases in the Southern BUS region.

In addition, the high O_2 – low I/Ca cases in the Southern BUS region may be related to the slow kinetics of iodide reoxidation. Estimated I⁻ oxidation rates range from 4 to 670 nM per year, whereas reduction of IO_3^- at an anoxic boundary is rapid (\sim 50 nM per hour) (Chance et al., 2014). Shelf waters in the Southern BUS (all water depths <200 m) were reported to have highly variable O_2 concentrations (10–400 µmol/kg) but low IO_3^- concentrations

W. Lu et al./Geochimica et Cosmochimica Acta xxx (2019) xxx-xxx

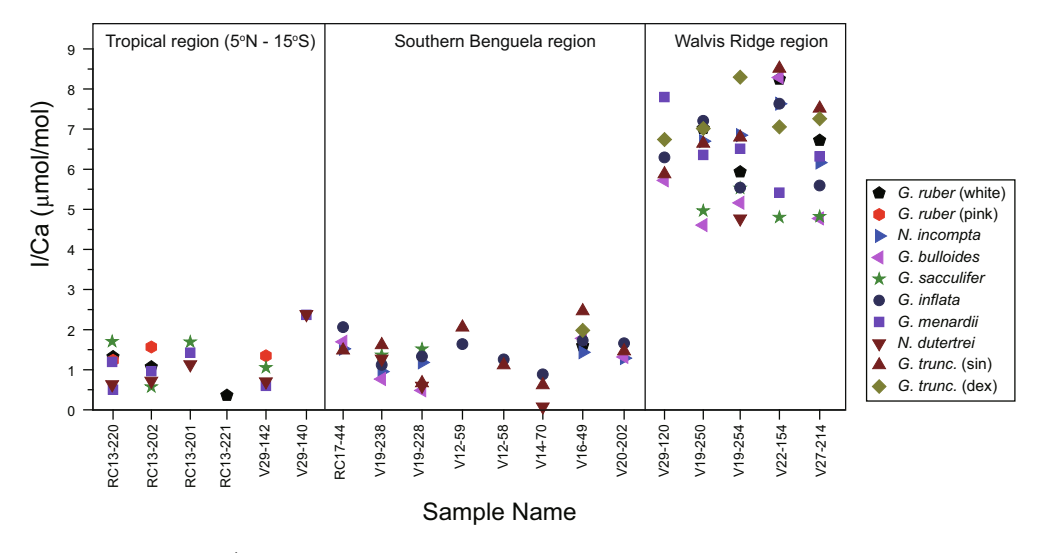


Fig. 4. Planktic I/Ca in core-top samples. The locations of the three regions are shown in Fig. 2a.

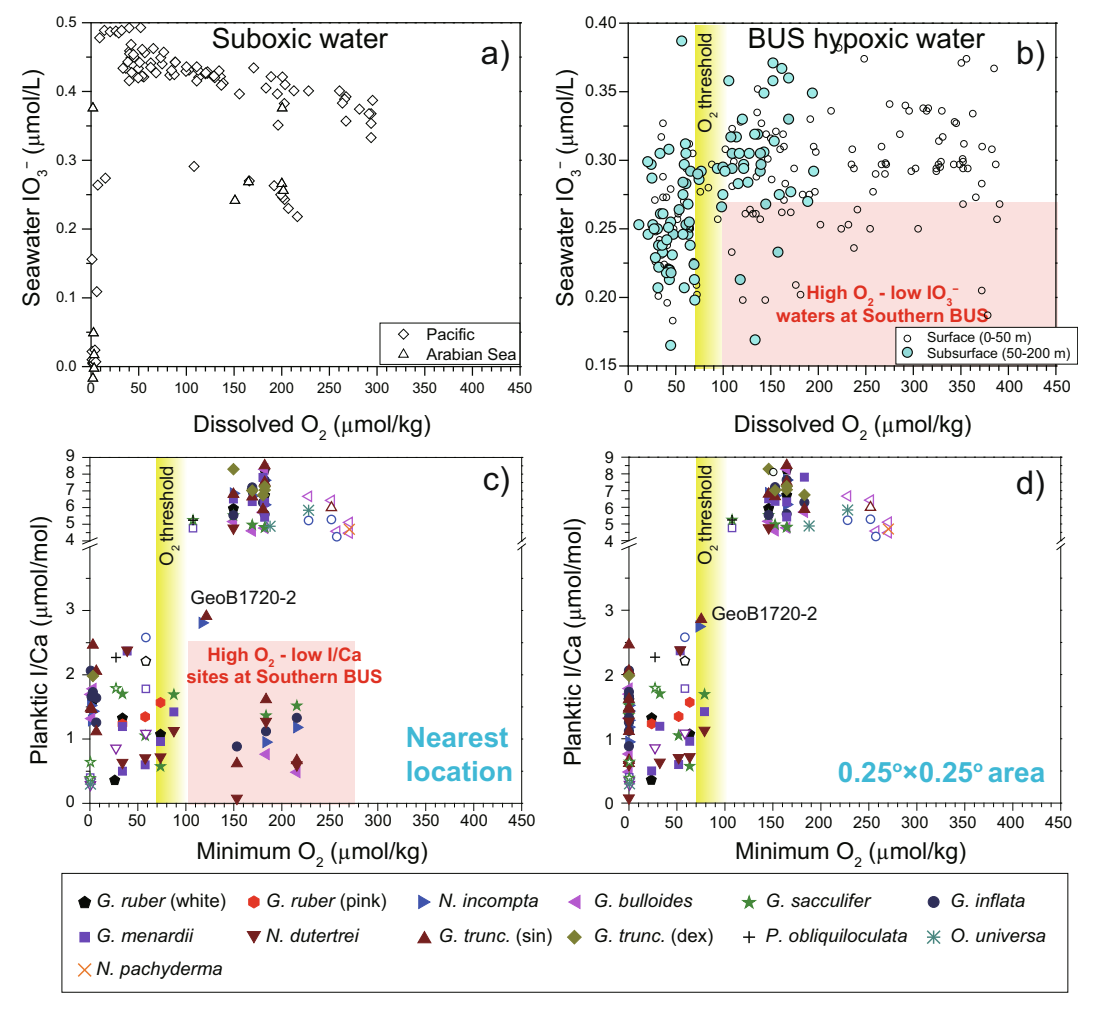


Fig. 5. (a) Dissolved IO_3^- vs. O_2 in the Pacific and Indian Oceans (Farrenkopf and Luther, 2002; Huang et al., 2005; Rue et al., 1997). (b) Dissolved IO_3^- vs. O_2 in shelf waters in Southern BUS (Chapman, 1983). Depths of all water samples were <200 m, locations are shown in the yellow box in Fig. 1. (c and d) Core-top planktic I/Ca vs. minimum O_2 concentrations in the water column derived from the nearest location and within $0.25^\circ \times 0.25^\circ$ area in WOD2013. Closed symbols indicate new data in this study, and open ones denote published data (Lu et al., 2016).

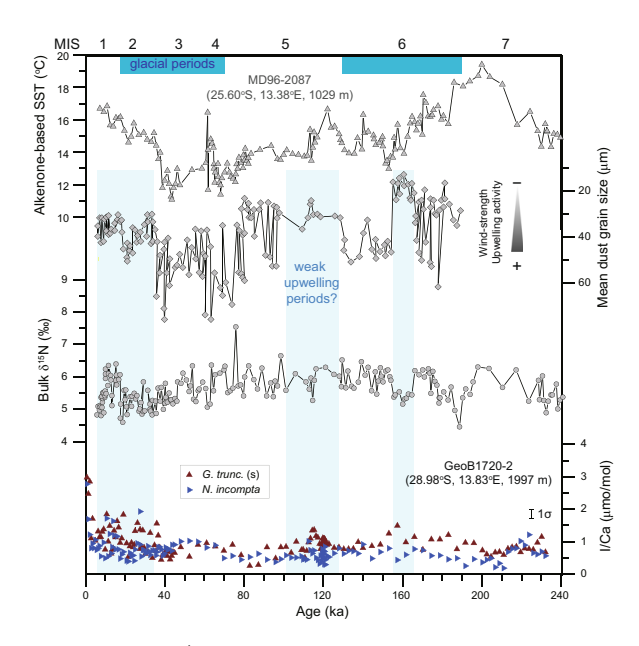


Fig. 6. Planktic I/Ca record at site GeoB1720-2 (this study), and alkenone-based SST, mean dust grain size (Pichevin et al., 2005a), and bulk $\delta^{15}N$ at site MD96-2087 (Pichevin et al., 2005b). Dark blue shadings indicate glacial periods, and light blue shadings indicate potential weak upwelling periods.

(\sim 0.25 μM) (Fig. 5b) (Chapman, 1983). Intense water column mixing in the shelf region of Southern BUS may bring bottom waters with low IO_3^- signals from peripheral locations into the photic zone, where the concentrations of nutrients and chlorophyll α are exceptionally high (Truesdale and Bailey, 2000). During this transport, oxygen concentrations may have begun to rise due to photosynthesis or mixing with O_2 -rich waters, but the IO_3^- concentration remained low due to the slow oxidation of I^- (Chapman, 1983; Truesdale and Bailey, 2000).

Central to these different scenarios for the occurrence of high O_2 - low I/Ca in the Southern BUS is the key concept that low foraminiferal I/Ca may reflect low O_2 conditions that vary on small space- and time-scales. To visualize such a spatial uncertainty, we plot I/Ca against minimum O_2 values within a $0.25^{\circ} \times 0.25^{\circ}$ area around each core-top location (Fig. 5). All core-top samples with low I/Ca in the Southern BUS come from a region where hypoxia occurs within 0.25° of the sample site (Fig. 5d). These results caution against the use of planktic I/Ca as a proxy for *in-situ* O_2 conditions, especially in settings with strong hydrographic gradients and mixing. However, we emphasize that these high O_2 – low I/Ca cases only occurred in the Southern BUS region with high spatial and temporal variability of O_2 , and not in the tropical and Walvis Ridge regions.

4.2. Planktic I/Ca as a hypoxia proxy

Water column IO_3^- and O_2 profiles from the core-top sites would provide the ideal constraints of the O_2 threshold driving the foraminiferal I/Ca signal. However, such modern seawater data are only available for a relatively small area from the Southern BUS (Chapman, 1983). In that

study, dissolved IO_3^- concentrations do not correlate with surface O_2 (depth < 50 m), but decrease rapidly when O_2 in subsurface waters (depth > 50 m) approaches ~70–100 µmol/kg (Fig. 5b). Similarly, our core-top I/Ca data exhibit abrupt decreases when minimum O_2 values drop to these levels, with the exception of the above described high O_2 – low I/Ca areas (Fig. 5c). This O_2 threshold for rapid IO_3^- or I/Ca decrease is generally consistent with the estimates based on globally-distributed core-top foraminifera (Lu et al., 2016).

We suggest that low planktic I/Ca can empirically indicate hypoxia in the upper water column, but it is not clear why planktic I/Ca responds to water column hypoxia, which warrants further discussion. We approach this question from two directions: the relationship between IO_3^- and O_2 in hypoxic waters, and the relation between IO_3^- reduction and denitrification.

Currently, water column data are insufficient to unambiguously demonstrate whether there is a uniform O₂ threshold for global seawater IO₃ reduction, and if there is such a threshold, at what concentration of O₂. IO₃⁻ concentrations rapidly decrease when waters become near suboxic ($[O_2] < 10 \,\mu\text{mol/kg}$) in the Pacific (Rue et al., 1997; Huang et al., 2005) and Indian oceans OMZs (Farrenkopf and Luther, 2002) (Fig. 5a). However, the Benguela data seem to indicate that IO₃⁻ reduction may occur at hypoxic conditions with somewhat higher oxygen levels $(O_2 < 70-100 \,\mu\text{mol/kg})$ (Fig. 5b), as also found over the shelf in the northern Gulf of Mexico (Chapman and Truesdale, 2011). Maybe, the O₂ threshold for seawater IO₃ reduction varies across different ocean basins, or there are other processes that control the balance between IO₃ and I in seawater (e.g., the uptake rate of IO₃ versus I by plankton, iodide oxidation rates vary in different oceans). Further work on seawater IO₃ and O₂ are required to discern these O₂ thresholds.

Since I/Ca and bulk $\delta^{15}N$ can indicate low-O₂ conditions in the upper water column and iodate reduction can be carried out by nitrate reductase, we explore some potential connections between IO₃ reduction and denitrification. Laboratory cultures have suggested that various types of algae and bacteria are able to reduce iodate to iodide in seawater (Farrenkopf et al., 1997; Waite and Truesdale, 2003; Chance et al., 2007), but the exact mechanisms remain unclear. Nitrate reductase enzymes have been speculated to be responsible for IO₃ reduction (Tsunogai and Sase, 1969; Wong and Hung, 2001), but no clear distinction has been made between assimilatory vs. dissimilatory nitrate reductases and their roles in seawater iodine speciation. Assimilatory nitrate reductases are generally associated with nitrate uptake in the euphotic zone (high O_2 water) (Wada and Hattori, 1990). Dissimilatory nitrate reductases are considered to function in suboxic conditions, although denitrifying bacteria isolated from marine sediment show nitrate reducing activity at O2 concentrations up to \sim 124 µmol/kg (Bonin et al., 1989). It may be worth further investigation into the prevalence and distribution of specific nitrate reductase enzymes responsible for IO₃⁻ reduction and their O₂ sensitivities coupled with water column IO₃ and O₂ concentrations.

Another possibility to explain a hypoxic threshold for rapid I/Ca decrease may involve anaerobic metabolism of microbes (including IO₃ reduction) in microenvironments of sinking organic aggregates in oxic-hypoxic water. Denitrification is often described as occurring in suboxic or anoxic waters only (Ulloa et al., 2012), but denitrification and even sulfate-reduction by microbes have been reported at $O_2 > 20 \,\mu\text{mol/kg}$ (Wolgast et al., 1998; Ganesh et al., 2014). Possibly, particle microenvironments in hypoxic waters may have sufficiently low O₂ concentrations to support anaerobic metabolism, including denitrification and sulfate reduction (Bianchi et al., 2018) and potentially iodate reduction. These low IO₃ signals formed in microenvironments could be subsequently released into ambient hypoxic seawater where the planktic foraminifera calcify. Such a scenario could be an explanation for IO₃ reduction in hypoxic water, and I/Ca may be sensitive to water column denitrification in microenvironments.

In summary, we suggest that planktic I/Ca remains an empirical proxy - low I/Ca values can reliably indicate the presence of hypoxia in the water column, in contrast to bulk sediment $\delta^{15}N$ as a proxy for denitrification in suboxic water. In future studies, foraminiferal I/Ca, paired O2 and iodate data from low O2 regions may improve the mechanistic understanding of the proxy and also the marine biogeochemistry of iodine. Iodate will not be used as oxidant until O₂ is significantly depleted, but iodate reduction may not necessarily occur in the habitat of calcifying organisms. The foraminiferal I/Ca signature for low O_2 reflects iodate reduction somewhere very close to the foraminiferal habitat. If the in-situ iodate level indeed is low, it can be caused by diffusion/advection and slow oxidation of iodide. On the other hand, culture experiments show that two modern planktic species (O. universa, symbiotic species, and G. bulloides, non-symbiotic species) can survive, add chambers, feed, and undergo gametogenesis in low-O₂ conditions (\sim 22 µmol/L) (Kuroyanagi et al., 2013). Some species (N. dutertrei and G. bulloides) can even survive episodic or temporary exposure to H₂S (<24 hr) (Kuroyanagi et al., 2019). We cannot rule out the possibility that planktic foraminifera may survive in hypoxic waters and directly record a low I/Ca signal. Such foraminifera culture experiments may also be helpful for testing vital effects in different species.

4.3. Planktic I/Ca downcore record in the BUS

We use the I/Ca values in N. incompta and G. truncatulinoides (sinistral) from core GeoB1720-2 from the Southeast Atlantic to reconstruct the upper water oxygenation history over the last 240 ka, and compare these results with $\delta^{15}N$ data from nearby site MD96-2087 (25.60°S, 13.38°E, 1029 m) (Pichevin et al., 2005b). The downcore I/Ca values are consistently low, <2.5 µmol/mol, over the last two glacial cycles (Fig. 6), indicating the persistent presence of hypoxic waters near the study site (e.g., within 0.25° × 0.25° area). It is possible that low IO_3^- water was advected to this site from nearby locations. Nutrient levels, indicated by bulk sediment $\delta^{15}N$ records from MD96-2087 (Fig. 6), likewise do not show a clear glacial-interglacial pattern

(Pichevin et al., 2005b). The narrow amplitude of this δ^{15} N record was interpreted to reflect that nitrate was never severely depleted over the shelf (Pichevin et al., 2005b). Thus the upwelling dynamics in the near-shore region of BUS may have persistently fueled relatively high levels of surface nutrient and subsurface hypoxia through glacialinterglacial oscillations, which remained a dominant oceanographic feature in this area. On the other hand, downcore records for excess Ba (Ba_{xs}) and the δ^{13} C difference between G. ruber (a summer calcifier) and N. incompta (calcifying below the mixed layer) ($\Delta \delta^{13}$ C) suggest changes in organic carbon export and upper ocean nutrient partitioning over the latter part of the last glacial cycle (Fig. 7). Given the very low I/Ca values, it is likely that subtle alternations of enhanced organic matter export and upper ocean mixing (high Ba_{xs}, low $\Delta\delta^{13}$ C) and lower organic matter export with more stratified surface waters (lower Ba_{xs} , higher $\Delta\delta^{13}C$) could maintain persistently oxygen-depleted subsurface waters during the past ~50 ka (Fig. 7). It is possible that such variations in export production were relatively small, thus insufficient to drive nutrient utilization ($\delta^{15}N$) and hypoxia patterns (I/Ca).

Upwelling strength may well have an impact on upper ocean oxygenation conditions in the region (Fig. 6). The alkenone-based SSTs at MD96-2087 (Fig. 6) did not exactly follow glacial-interglacial cycles, but were strongly influenced by upwelling activity and wind-strength, as recorded by dust grain size distributions (Pichevin et al., 2005a). Weak upwelling periods at MD96-2087 coincided temporally with relatively weaker hypoxia as indicated by higher I/Ca of *G. truncatulinoides* in GeoB1720-2 (Fig. 6). Comparing I/Ca records of hypoxic extent with independent proxies for upwelling strengths may be an intriguing future research direction.

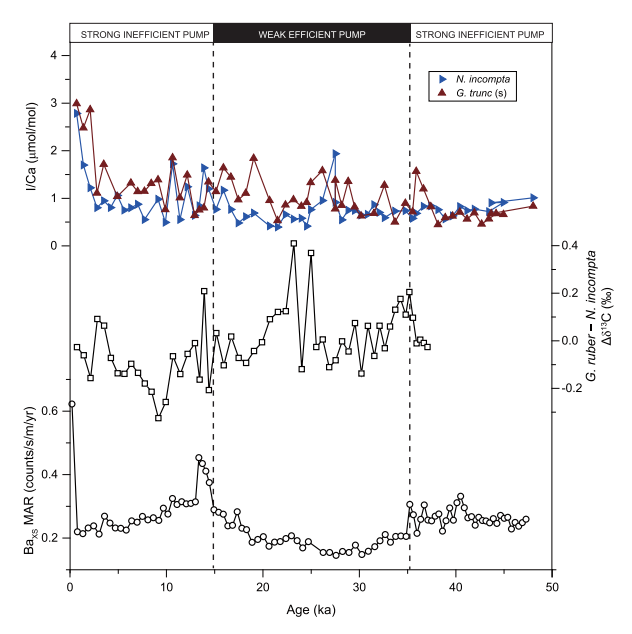


Fig. 7. Planktic I/Ca, the δ^{13} C difference between *G. ruber* and *N. incompta*, and excess Ba mass accumulation rates (MAR) records at core GeoB1720-2 during the last 50 ka.

5. CONCLUSIONS

New core-top I/Ca data in planktic foraminifera from the Southeast Atlantic Ocean are consistent with previous studies, generally showing low I/Ca corresponding to low oxygen in the upper ocean. This study thus further establishes planktic I/Ca as an empirical proxy for hypoxic conditions ($O_2 < \sim 70-100 \,\mu\text{mol/kg}$) in the Southeast Atlantic. Data from the Southern Benguela region show a more complex pattern, and indicate limitations on the use of planktic I/Ca as an *in-situ* O₂ proxy for the foraminiferal habitat. In areas with intense mixing/upwelling, seawater signals may be affected by short-term O2 variability and/or potential transport of hypoxia signals at nearby locations due to the slow kinetics of iodide re-oxidation. Future work are required to better understand the mechanistic relationship between iodate, O2 and foraminiferal I/Ca. The downcore planktic I/Ca record at site GeoB1720-2 suggests that there were no significant glacial-interglacial variations in upper water hypoxic extent within the BUS during the last 240 ka, consistent with bulk δ^{15} N signals at a nearby site. In this region, relatively small temporal variations in I/Ca shows a potential connection with upwelling intensity.

ACKNOWLEDGEMENTS

We thank Lamont-Doherty Core Repository for providing core-top materials, the Bremen GeoB core repository for curating and providing material from core GeoB1720-2. We also thank Simona Nicoara at Open University for the $\delta^{18}O$ analysis at core GeoB1720-2. This manuscript greatly benefited from comments by three anonymous reviewers. The O_2 data in Fig. 5b has been supplied by the Southern African Data Centre for Oceanography (http://sadco.csir.co.za/). This work is supported by NSF grants OCE-1232620, OCE-1736542 and EAR-1349252 (to ZL), and OCE-1736538 (ET).

APPENDIX A. SUPPLEMENTARY MATERIAL

Supplementary data to this article can be found online at https://doi.org/10.1016/j.gca.2019.10.025.

REFERENCES

- Altabet M. A., Pilskaln C., Thunell R., Pride C., Sigman D., Chavez F. and Francois R. (1999) The nitrogen isotope biogeochemistry of sinking particles from the margin of the Eastern North Pacific. *Deep Sea Res. Part I* 46, 655–679.
- Anand P., Elderfield H. and Conte M. H. (2003) Calibration of Mg/Ca thermometry in planktonic foraminifera from a sediment trap time series. *Paleoceanography* 18, 1050.
- Bianchi D., Weber T. S., Kiko R. and Deutsch C. (2018) Global niche of marine anaerobic metabolisms expanded by particle microenvironments. *Nat. Geosci.* 11, 263–268.
- Bonin P., Gilewicz M. and Bertrand J. (1989) Effects of oxygen on each step of denitrification on Pseudomonas nautica. *Can. J. Microbiol.* 35, 1061–1064.
- Boyer T. P., Antonov J. I., Baranova O. K., Coleman C., Garcia H.
 E., Grodsky A., Johnson D. R., Locarnini R. A., Mishonov A.
 V., O'Brien T. D., Paver C. R., Reagan J. R., Seidov D.,
 Smolyar I. V. and Zweng M. M. (2013) World Ocean Database
 2013. NOAA Atlas NESDIS 72, Silver Spring, MD, 209 p.

- Chance R., Baker A. R., Carpenter L. and Jickells T. D. (2014) The distribution of iodide at the sea surface. *Environ. Sci. Processes Impacts* 16, 1841–1859.
- Chance R., Malin G., Jickells T. and Baker A. R. (2007) Reduction of iodate to iodide by cold water diatom cultures. *Mar. Chem.* 105, 169–180.
- Chapman P. (1983) Changes in iodine speciation in the Benguela Current upwelling system. *Deep Sea Res. Part A Oceanogr. Res. Pap.* **30**, 1247–1259.
- Chapman P. and Shannon L. (1985) The Benguela ecosystem. Part II. Chemistry and related processes. *Oceanogr. Mar. Biol. Annu. Rev.* **23**, 183–251.
- Chapman P. and Truesdale V. W. (2011) Preliminary evidence for iodate reduction in bottom waters of the Gulf of Mexico during an hypoxic event. *Aguat. Geochem.* 17, 671–695.
- Dickson A. J., Beer C. J., Dempsey C., Maslin M. A., Bendle J. A., McClymont E. L. and Pancost R. D. (2009) Oceanic forcing of the Marine Isotope Stage 11 interglacial. *Nat. Geosci.* 2, 428.
- Dickson A. J., Leng M. J., Maslin M. A., Sloane H. J., Green J., Bendle J. A., McClymont E. L. and Pancost R. D. (2010) Atlantic overturning circulation and Agulhas leakage influences on southeast Atlantic upper ocean hydrography during marine isotope stage 11. *Paleoceanography* 25, PA3208.
- Farmer E. C., Demenocal P. B. and Marchitto T. M. (2005) Holocene and deglacial ocean temperature variability in the Benguela upwelling region: Implications for low-latitude atmospheric circulation. *Paleoceanography* 20, PA2018.
- Farrenkopf A. M., Dollhopf M. E., Chadhain S. N., Luther, III, G. W. and Nealson K. H. (1997) Reduction of iodate in seawater during Arabian Sea shipboard incubations and in laboratory cultures of the marine bacterium Shewanella putrefaciens strain MR-4. *Mar. Chem.* 57, 347–354.
- Farrenkopf A. M. and Luther G. W. (2002) Iodine chemistry reflects productivity and denitrification in the Arabian Sea: evidence for flux of dissolved species from sediments of western India into the OMZ. *Deep Sea Res. Part II* 49, 2303–2318.
- Feng X. and Redfern S. A. (2018) Iodate in calcite, aragonite and vaterite CaCO3: Insights from first-principles calculations and implications for the I/Ca geochemical proxy. *Geochim. Cos-mochim. Acta* 236, 351–360.
- Galbraith E. D. and Jaccard S. L. (2015) Deglacial weakening of the oceanic soft tissue pump: global constraints from sedimentary nitrogen isotopes and oxygenation proxies. *Quat. Sci. Rev.* 109, 38–48.
- Galbraith E. D., Kienast M., Albuquerque A. L., Altabet M. A., Batista F., Bianchi D., Calvert S. E., Contreras S., Crosta X. and De Pol-Holz R. (2013) The acceleration of oceanic denitrification during deglacial warming. *Nat. Geosci.* 6, 579.
- Galbraith E. D., Kienast M., Jaccard S. L., Pedersen T. F., Brunelle B. G., Sigman D. M. and Kiefer T. (2008) Consistent relationship between global climate and surface nitrate utilization in the western subarctic Pacific throughout the last 500 ka. *Paleoceanogr. Paleoclimatol.* 23, PA2212.
- Ganesh S., Parris D. J., DeLong E. F. and Stewart F. J. (2014) Metagenomic analysis of size-fractionated picoplankton in a marine oxygen minimum zone. *ISME J.* **8**, 187.
- Hoogakker B. A., Lu Z., Umling N., Jones L., Zhou X., Rickaby R. E., Thunell R., Cartapanis O. and Galbraith E. (2018)
 Glacial expansion of oxygen-depleted seawater in the eastern tropical Pacific. *Nature* 562, 410.
- Huang Z., Ito K., Morita I., Yokota K., Fukushi K., Timerbaev A. R., Watanabe S. and Hirokawa T. (2005) Sensitive monitoring of iodine species in sea water using capillary electrophoresis: vertical profiles of dissolved iodine in the Pacific Ocean. *J. Environ. Monit.* 7, 804–808.

- Hutchings L., Van der Lingen C., Shannon L., Crawford R., Verheye H., Bartholomae C., Van der Plas A., Louw D., Kreiner A. and Ostrowski M. (2009) The Benguela Current: an ecosystem of four components. *Prog. Oceanogr.* 83, 15–32.
- Jarre A., Hutchings L., Crichton M., Wieland K., Lamont T., Blamey L., Illert C., Hill E. and van den Berg M. (2015) Oxygen-depleted bottom waters along the west coast of South Africa, 1950–2011. Fish. Oceanogr. 24, 56–73.
- Kuroyanagi A., da Rocha R. E., Bijma J., Spero H. J., Russell A. D., Eggins S. M. and Kawahata H. (2013) Effect of dissolved oxygen concentration on planktonic foraminifera through laboratory culture experiments and implications for oceanic anoxic events. *Mar. Micropaleontol.* 101, 28–32.
- Kuroyanagi A., Toyofuku T., Nagai Y., Kimoto K., Nishi H., Takashima R. and Kawahata H. (2019) Effect of euxinic conditions on planktic foraminifers: culture experiments and implications for past and future environments. *Paleoceanogr. Paleoclimatol.* 34, 54–62.
- Lamont T., Hutchings L., Van Den Berg M., Goschen W. and Barlow R. (2015) Hydrographic variability in the St. Helena Bay region of the southern Benguela ecosystem. *J. Geophys. Res. Oceans* 120, 2920–2944.
- Lisiecki L. E. and Raymo M. E. (2005) A Pliocene-Pleistocene stack of 57 globally distributed benthic δ18O records. *Paleoceanography* **20**, PA1003.
- Lu W., Ridgwell A., Thomas E., Hardisty D., Luo G., Algeo T., Saltzman M., Gill B., Shen Y., Ling H., Edwards C., Whalen M., Zhou X., Gutchess K., Jin L., Rickaby R., Jenkyns H., Lyons T., Lenton T., Kump L. and Lu Z. (2018) Late inception of a resiliently oxygenated upper ocean. *Science* 361, 174–177.
- Lu Z., Hoogakker B. A., Hillenbrand C.-D., Zhou X., Thomas E., Gutchess K. M., Lu W., Jones L. and Rickaby R. E. (2016) Oxygen depletion recorded in upper waters of the glacial Southern Ocean. *Nat. Commun.* 7, 11146.
- Lu Z., Jenkyns H. C. and Rickaby R. E. (2010) Iodine to calcium ratios in marine carbonate as a paleo-redox proxy during oceanic anoxic events. *Geology* 38, 1107–1110.
- McKay C., Filipsson H., Romero O., Stuut J. B. and Björck S. (2016) The interplay between the surface and bottom water environment within the Benguela Upwelling System over the last 70 ka. *Paleoceanography* 31, 266–285.
- Mollenhauer G., Eglinton T., Ohkouchi N., Schneider R., Müller P., Grootes P. and Rullkötter J. (2003) Asynchronous alkenone and foraminifera records from the Benguela Upwelling System. *Geochim. Cosmochim. Acta* 67, 2157–2171.
- Mollenhauer G., Schneider R. R., Müller P. J., Spieß V. and Wefer G. (2002) Glacial/interglacial variablity in the Benguela upwelling system: Spatial distribution and budgets of organic carbon accumulation. Glob. Biogeochem. Cycl. 16, 1134.
- Pichevin L., Cremer M., Giraudeau J. and Bertrand P. (2005a) A 190 ky record of lithogenic grain-size on the Namibian slope: forging a tight link between past wind-strength and coastal upwelling dynamics. *Mar. Geol.* 218, 81–96.
- Pichevin L., Martinez P., Bertrand P., Schneider R., Giraudeau J. and Emeis K. (2005b) Nitrogen cycling on the Namibian shelf and slope over the last two climatic cycles: Local and global forcings. *Paleoceanography* **20**, PA2006.

- Pitcher G. C., Probyn T. A., du Randt A., Lucas A., Bernard S., Evers-King H., Lamont T. and Hutchings L. (2014) Dynamics of oxygen depletion in the nearshore of a coastal embayment of the southern Benguela upwelling system. *J. Geophys. Res. Oceans* 119, 2183–2200.
- Podder J., Lin J., Sun W., Botis S., Tse J., Chen N., Hu Y., Li D., Seaman J. and Pan Y. (2017) Iodate in calcite and vaterite: Insights from synchrotron X-ray absorption spectroscopy and first-principles calculations. *Geochim. Cosmochim. Acta* 198, 218–228
- Robinson R., Martinez P., Pena L. and Cacho I. (2009) Nitrogen isotopic evidence for deglacial changes in nutrient supply in the eastern equatorial Pacific. *Paleoceanography* **24**, PA4213.
- Romero O., Crosta X., Kim J.-H., Pichevin L. and Crespin J. (2015) Rapid longitudinal migrations of the filament front off Namibia (SE Atlantic) during the past 70 kyr. *Glob. Planet. Change* 125, 1–12.
- Rue E. L., Smith G. J., Cutter G. A. and Bruland K. W. (1997) The response of trace element redox couples to suboxic conditions in the water column. *Deep Sea Res. Part I* 44, 113–134.
- Schlitzer, R., 2018. Ocean Data View (http://odv.awi.de).
- Schmidtko S., Stramma L. and Visbeck M. (2017) Decline in global oceanic oxygen content during the past five decades. *Nature* 542, 335.
- Shannon L. and Nelson G. (1996) *The Benguela: Large Scale Features and Processes and System Variability*. Springer, The South Atlantic, pp. 163–210.
- Stramma L. and England M. (1999) On the water masses and mean circulation of the South Atlantic Ocean. *J. Geophys. Res. Oceans* **104**, 20863–20883.
- Truesdale V. and Bailey G. (2000) Dissolved iodate and total iodine during an extreme hypoxic event in the Southern Benguela system. *Estuar. Coast. Shelf Sci.* **50**, 751–760.
- Tsunogai S. and Sase T. (1969) Formation of iodide-iodine in the ocean. *Deep Sea Res. Oceanogr. Abstr.* **16**(5), 489–496.
- Ulloa O., Canfield D. E., DeLong E. F., Letelier R. M. and Stewart F. J. (2012) Microbial oceanography of anoxic oxygen minimum zones. *Proc. Natl. Acad. Sci.* 109, 15996–16003.
- Wada E. and Hattori A. (1990) Nitrogen in the Sea: Forms, Abundance, and Rate Processes. CRC Press.
- Waite T. J. and Truesdale V. W. (2003) Iodate reduction by Isochrysis galbana is relatively insensitive to de-activation of nitrate reductase activity—are phytoplankton really responsible for iodate reduction in seawater? *Mar. Chem.* 81, 137–148.
- Wolgast D., Carlucci A. and Bauer J. (1998) Nitrate respiration associated with detrital aggregates in aerobic bottom waters of the abyssal NE Pacific. *Deep Sea Res. Part II* **45**, 881–892.
- Wong G. T. and Hung C.-C. (2001) Speciation of dissolved iodine: integrating nitrate uptake over time in the oceans. *Cont. Shelf Res.* 21, 113–128.
- Zhou X., Thomas E., Rickaby R. E., Winguth A. M. and Lu Z. (2014) I/Ca evidence for upper ocean deoxygenation during the PETM. *Paleoceanography* 29, 964–975.

Associate Editor: Jennifer Morford